

# Microscopic modeling of magnetic-field effects on charge transport in organic semiconductors

A. J. Schellekens,<sup>\*</sup> W. Wagemans, S. P. Kersten, P. A. Bobbert, and B. Koopmans

*Department of Applied Physics, Center for NanoMaterials (cNM), Eindhoven University of Technology, P.O.Box 513,  
5600 MB, Eindhoven, The Netherlands*

(Received 24 January 2011; revised manuscript received 26 May 2011; published 9 August 2011)

The stochastic Liouville equation is applied to the field of organic magnetoresistance to perform detailed microscopic calculations on the different proposed models. By adapting this equation, the influence of a magnetic field on the current in bipolaron, electron-hole pair, and triplet models is calculated. The simplicity and wide applicability of the stochastic Liouville equation makes it a powerful tool for interpreting experimental results on magnetoresistance measurements in organic semiconductors. New insights are gained on the influence of hopping rates and disorder on the magnetoresistance.

DOI: [10.1103/PhysRevB.84.075204](https://doi.org/10.1103/PhysRevB.84.075204)

PACS number(s): 72.80.Le, 73.61.Ph

## I. INTRODUCTION

A large magnetoresistance in disordered organic semiconductors has been discovered in materials without any ferromagnetic electrodes.<sup>1,2</sup> This effect, commonly referred to as organic magnetoresistance (OMAR), can be as large as 10% at room temperature and magnetic fields of only 10 mT, making it potentially suitable for future applications. Since its discovery, various mechanisms to explain the large magnetoresistance have been proposed by various authors.<sup>3–5</sup> However, none of them unambiguously explain all the experimental results. Although the models for OMAR are based on different processes, ranging from bipolaron formation<sup>5</sup> to recombination of electron-hole (e–h) pairs<sup>3</sup> and detrapping of charges by triplet excitons,<sup>4</sup> there is also a strong similarity between these mechanisms. In the proposed models an applied magnetic field alters the spin-dependent reactions between two particles, thereby changing the current through the organic devices.

For one of the models, namely the bipolaron model, explicit calculations have been performed by means of Monte Carlo simulations<sup>5</sup> and by considering a simple two-site model.<sup>6</sup> However, for the other models explicit, quantum-mechanical calculations are lacking, and the interpretation of experimental results is often based on qualitative reasoning and/or simplified rate equations. Moreover, various OMAR-related phenomena are claimed to be observed in literature, like spin mixing by a difference in  $g$  factors of electrons and holes<sup>7,8</sup> or high-field effects caused by triplet excitons.<sup>9–11</sup> Also in those cases, we feel that a more explicit quantum-mechanical treatment would be beneficial.

In this paper we use a simple master equation for open quantum systems, based on the density-matrix formalism, capable of describing different types of spin-spin reactions in organic semiconductors. This master equation, often referred to as the stochastic Liouville equation,<sup>12</sup> is adapted to perform detailed microscopic calculations on the various OMAR models, making it an extremely useful tool for interpreting experimental results.

We will start this paper by introducing the stochastic Liouville equation, after which calculations on four different magnetic-field-dependent spin-spin reactions are performed: bipolaron formation, e–h pair recombination, detrapping of charges by triplet excitons, and the mutual annihilation of

triplet excitons. Calculations are focused on the influence of the spin-spin reactions on the current, but all of them could potentially lead to a similar magnetic-field effect on, for example, the electroluminescence or the photogenerated current.

## II. STOCHASTIC LIOUVILLE EQUATION

It will be shown that to perform calculations on spin-spin reactions in organic semiconductors the density-matrix formalism is invaluable. First, spin pairs are created in random spin states (with the exception of photoexcitations), i.e., the mutual orientation of the spins on pair formation is random, demanding a statistical approach of the quantum system. Second, incoherent hopping of particles also requires calculations to be performed on an ensemble of spin states, properly described by a density matrix. As a starting point we therefore consider an ensemble of  $N$  spin pairs in the respective spin states  $\Psi_n$ . The dynamics of such an ensemble can be described by introducing a density operator:

$$\rho = \frac{1}{N} \sum_{n=1}^N |\Psi_n\rangle\langle\Psi_n|. \quad (1)$$

By choosing an orthonormal basis  $\phi_i$ , we can define the density matrix as follows:

$$\rho_{i,j} = \langle\phi_i|\rho|\phi_j\rangle. \quad (2)$$

The diagonal elements of  $\rho$  give the probability of finding the system in the corresponding basis states. The density matrix fully describes the state of the ensemble, and the expectation values for any observable can be obtained from it. The time evolution of the ensemble is easily derived from the Schrödinger equation and is given by the Liouville equation:

$$\frac{\partial\rho}{\partial t} = -\frac{i}{\hbar}[H,\rho], \quad (3)$$

where  $H$  is the spin-pair Hamiltonian and the square brackets denote the commutator. For the spin-dependent reactions in organic semiconductors we would like to model, usually two types of interactions are present in the Hamiltonian. The first type of interactions are nondissipative interactions under which the ensemble coherently evolves in time, such as the Zeeman, exchange, and/or hyperfine interactions. These

interactions can be simply taken into account by using an appropriate spin Hamiltonian. On the other hand there are dissipative interactions that incoherently create or destroy spin states under the influence of interactions with an environment. An example of such an interaction is phonon-assisted bipolaron formation, removing polaron pairs from an ensemble of such pairs. To properly describe these dissipative interactions with the environment, the theory for open quantum systems should be used.

In the literature a master equation governing the system dynamics has been introduced with considerable success in different fields of research, ranging from delayed fluorescence in organic semiconducting crystals to laser theory.<sup>13,14</sup> This equation was first introduced by Scully and Lamb and is often referred to as the stochastic Liouville equation:<sup>14</sup>

$$\frac{\partial \rho}{\partial t} = -\frac{i}{\hbar}[H, \rho] - \frac{1}{2}\{\Lambda, \rho\} + \Gamma. \quad (4)$$

The first term on the right-hand side of Eq. (4) is the Liouville term from Eq. (3) and corresponds to the coherent evolution of the spin pairs in absence of interactions with the environment. The second term is a dissipative term, (spin selectively) removing spin pairs from the system, where the curly braces denote the anticommutator and  $\Lambda$  is a projection operator projecting on the spin subspace from which reactions are allowed. The role of the anticommutator is discussed by Haberkorn and preserves the hermiticity of  $\rho$ .<sup>15</sup> The last term is a source term, adding spin pairs to the system.

Although Eq. (4) was originally introduced on a phenomenological basis, it can be shown that incoherent spin-dependent reactions by interactions with a thermal bath are taken into account correctly by the anticommutator of  $\Lambda$  and  $\rho$ .<sup>16</sup>  $\rho$  in Eq. (4) is strictly speaking no density matrix, as the trace of the matrix is not equal to one.  $\rho$  is merely a measure for the amount of spin pairs in the system, as the reaction products are neglected. The statistical interpretation of  $\rho$  can always be obtained by calculating the reduced density operator for the spin pairs simply by dividing  $\rho$  by its trace.

Equation (4) can be used to describe a system where pair states are created by  $\Gamma$ , states are (spin selectively) destroyed or removed by  $\Lambda$ , and states evolve in time according to the spin-pair Hamiltonian  $H$ . It is this equation that will serve as a starting point for the calculations of the different spin-spin reactions in disordered organic semiconductors assumed to be responsible for the observed magnetoresistance. By simply using the correct spin Hamiltonian and slightly adapting the stochastic Liouville equation the different OMAR models can be implemented.

Spin chemistry,<sup>17</sup> a field closely related to that of OMAR, is a primary example of how theoretical calculations exploiting the stochastic Liouville equation can be used to support the interpretation of experiments on magnetic-field-dependent reactions and gain further insight into their underlying mechanisms. A detailed review of the field is given by Steiner and Ulrich.<sup>18</sup> In the review the authors concluded that there are many different mechanisms through which a magnetic field can modify chemical reaction rates. It is likely that the same holds for OMAR, i.e., all the proposed models can potentially alter the current in organic semiconductors. The type of device and the operating conditions determine whether

a specific model is the dominant mechanism contributing to the magnetoresistance. For this reason, the goal of the presented calculations is not to falsify any of the proposed models, but to elucidate their basic properties, which can be used to discriminate between the models in specific experiments. In this perspective, calculations are performed on the most common spin-dependent reactions used to explain OMAR, namely bipolaron formation, e-h pair recombination, and triplet exciton reactions.

### III. BIPOLARON MODEL

#### A. Basic concepts

One of the models for OMAR has been proposed by Bobbert *et al.*<sup>5</sup> In this model two charges with equal sign can form a bipolaron as an intermediate state depending on the mutual orientation of the spins. This bipolaron formation rate depends on the applied magnetic field, as the magnetic field alters the evolution of the individual spins in the pair. By changing the bipolaron formation rate the current is also changed, as certain sites are effectively blocked if bipolaron formation is not possible.

The basic microscopic concept of the bipolaron model is shown in Fig. 1. When a polaron pair is formed, the individual spins precess around their local magnetic fields. This local magnetic field is a sum of the applied magnetic field and the local random hyperfine fields. The latter originate from the coupling of the polaron spins to the spins of the hydrogen protons in the organic molecules. Schulten and Wolynes<sup>19</sup> have shown that interactions of a single polaron with a sufficiently large number of hydrogen protons can be approximated by a static random magnetic field. The  $x$ ,  $y$ , and  $z$  components of this static hyperfine field are normally distributed around zero with a standard deviation  $\sigma_{\text{hf}}$  corresponding to the average hyperfine-field strength. The resulting polaron-pair Hamiltonian is the following:

$$\begin{aligned} H &= H_{Z,\alpha} + H_{Z,\beta} + H_{\text{hf},\alpha} + H_{\text{hf},\beta}, \\ H_{Z,i} &= \frac{g\mu_B}{\hbar} \vec{B}_{\text{app}} \cdot \vec{S}_i, \\ H_{\text{hf},i} &= \frac{g\mu_B}{\hbar} \vec{B}_{\text{hf},i} \cdot \vec{S}_i, \end{aligned} \quad (5)$$

where  $g$  is the polaron  $g$  factor, which is  $\approx 2$ ,  $\mu_B$  is the Bohr magneton,  $\hbar$  is the reduced Planck constant,  $\vec{B}_{\text{app}}$  is the applied magnetic field,  $\vec{B}_{\text{hf},\alpha}$  and  $\vec{B}_{\text{hf},\beta}$  are the hyperfine fields

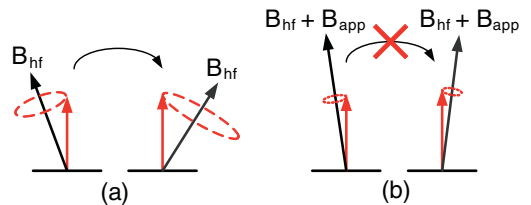


FIG. 1. (Color online) (a) Bipolaron formation without a field. Local hyperfine fields mix the singlet and triplet states. (b) Bipolaron formation in a large applied field. The external magnetic field suppresses the hyperfine induced mixing of the singlet and triplet states, reducing the bipolaron formation probability.

experienced by the two polarons in a pair, and  $\vec{S}_\alpha$  and  $\vec{S}_\beta$  are the spin operators of the individual polarons.

In the absence of an applied magnetic field, a pair of polarons on neighboring localized sites that is formed in the triplet state can obtain a singlet character, as both polarons precess around a small static random magnetic field, which changes the mutual orientation of the spins. Only when the polaron pair has a singlet component it is possible for one of the polarons to hop to the neighboring site and form an intermediate bipolaron before hopping further through the device. This process is schematically depicted in Fig. 1(a). However, on applying an external magnetic field, the random hyperfine fields are suppressed and the individual spins precess around identical local magnetic fields, hence suppressing mixing. This suppression of mixing leads to a decrease of the bipolaron formation rate, as depicted in Fig. 1(b).

In passing, we note that we focus here on the simplest model, neglecting effects like an exchange, dipolar, and spin-orbit interaction. Adding the first two is a straightforward extension of the polaron-pair Hamiltonian; however, a detailed discussion is given elsewhere.<sup>20</sup> Also the spin-orbit interaction (SOI) could potentially be included in the polaron-pair Hamiltonian; however, we neglected the SOI for two reasons. First, this interaction is expected to be small for the commonly used light organic materials. This is supported by the observation that the hyperfine interaction is the dominant spin-relaxation mechanism in organic spin valves.<sup>21</sup> Second, adding the SOI requires that the orbital degrees of freedom be taken into account. This would complicate the presented calculations dramatically, which is beyond the scope of the work presented in this paper.

### B. Two-site model: Density-matrix calculations

To calculate the magnetic-field dependence of bipolaron formation, a model system will be used based on the two-site model proposed by Wagemans *et al.*,<sup>6</sup> which has shown that many effects observed in OMAR can be obtained by considering only two characteristic sites. By adapting the stochastic Liouville equation a full density-matrix description of the two-site model will be given, making it possible to study properties of the bipolaron model in the regime where the hopping frequency  $\omega_{\text{hop}}$  is in the order of or larger than the hyperfine precession frequency  $\omega_{\text{hf}} = g\mu_B\sigma_{\text{hf}}/\hbar$ . Also other interactions are easily added to the spin-pair Hamiltonian, making it possible to study effects like an increased spin mixing due to a difference in  $g$  factors of the polarons, and interactions like a dipole coupling or an exchange interaction.<sup>20</sup>

A schematic drawing of the two-site model is depicted in Fig. 2. In this model there are two molecular sites,  $\alpha$  and  $\beta$ , with their local hyperfine fields  $\vec{B}_{\text{hf},\alpha}$  and  $\vec{B}_{\text{hf},\beta}$ . Sites  $\alpha$  and  $\beta$  are, respectively, at most and at least singly occupied. If site  $\alpha$  is unoccupied, a polaron can hop from the environment to site  $\alpha$  with a rate  $r_{e\alpha}$ . When site  $\alpha$  is occupied by a polaron it will precess around the local magnetic field. This polaron can now do two things: either hop directly to the environment with a rate  $r_{\alpha e}$  or form a bipolaron by hopping to site  $\beta$  with a rate  $P_S r_{\alpha\beta}$ , where  $P_S$  is the probability of finding the polarons on sites  $\alpha$  and  $\beta$  in a singlet configuration. After a bipolaron is

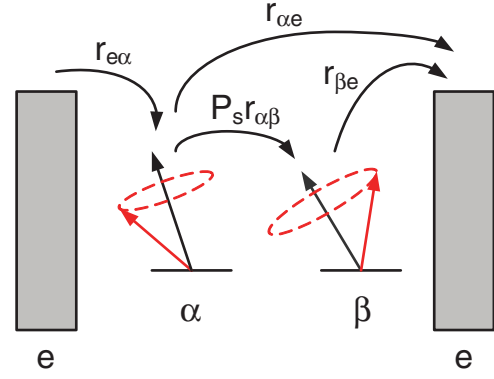


FIG. 2. (Color online) Two-site model as presented by Wagemans *et al.*<sup>6</sup> The symbols are explained in the text.

formed, it will dissociate with a rate  $r_{\beta e}$  by one of the polarons hopping from site  $\beta$  to the environment. The current through the system is defined as the total flow of polarons from the environment to site  $\alpha$ .

A full density-matrix description of the two-site model is given by an adapted stochastic Liouville equation:

$$\begin{aligned} \frac{\partial \rho}{\partial t} = & -\frac{i}{\hbar} [H, \rho] - \frac{1}{2} (r_{\alpha e} + r_{\alpha\beta}) \{\Lambda_S, \rho\} \\ & - \frac{1}{2} r_{\alpha e} \{\Lambda_T, \rho\} + \frac{1}{4} r_{e\alpha} (1 - \text{Tr}(\rho)) \Gamma, \end{aligned} \quad (6)$$

where  $\Lambda_S$  and  $\Lambda_T$  are projection operators on, respectively, the singlet and triplet states, and  $\Gamma$  is the identity matrix corresponding to the creation of spin pairs with a fully random orientation. Note that we set  $r_{\beta e} = \infty$  to simplify the calculations. Equation (6) keeps track of the polaron-pair spin states, where the trace of  $\rho$  represents the occupation of site  $\alpha$ . The current through the system is thus given by  $I = r_{e\alpha} (1 - \text{Tr}(\rho))$ . As OMAR is a steady-state phenomenon we are interested in the solutions of  $\partial \rho / \partial t = 0$ . By solving Eq. (6) the current for a particular applied field can be calculated. Finally, the magnetoconductance (MC) can be evaluated by calculating

$$\text{MC} = \frac{I(B) - I(0)}{I(0)} 100\%. \quad (7)$$

The original two-site model<sup>6</sup> has been developed for the limit  $\omega_{\text{hf}}/\omega_{\text{hop}} \gg 1$ , i.e., for the slow-hopping regime. We have checked and confirmed that the obtained line shapes from the density-matrix calculations in this regime are identical to the ones from the original model. In this paper we will focus on elucidating properties of the different models that are not reported in literature; hence we will focus on calculating properties of the bipolaron model in the intermediate- and fast-hopping regime.

### C. Hopping-rate dependence

All MC line shapes reported in the literature are calculated for  $\omega_{\text{hf}}/\omega_{\text{hop}} \gg 1$ , i.e., when mixing is much faster than hopping. In this section we will show how the MC and linewidths change as a function of the hopping rate.

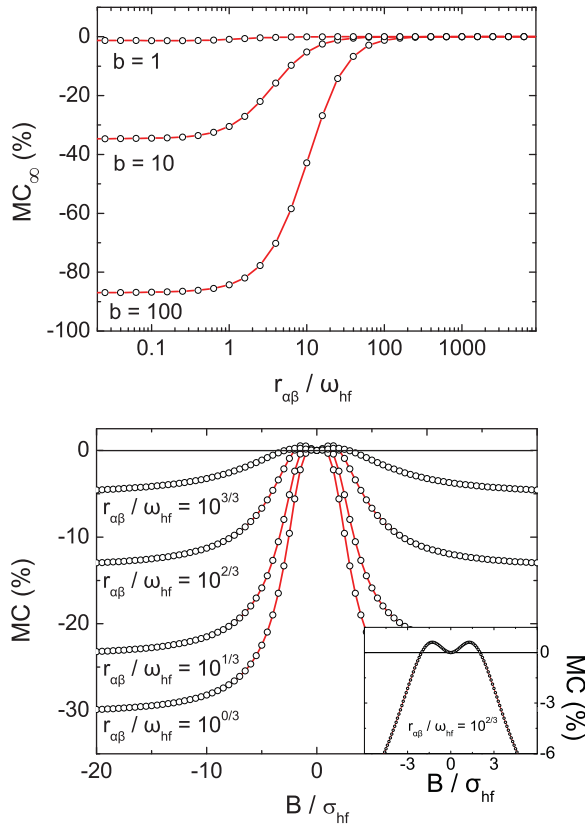


FIG. 3. (Color online) (a) Influence of the hopping rate  $r_{\alpha\beta}$  on the magnetoconductance in infinitely large fields. On increasing the hopping rate the MC is effectively quenched. (b) MC line shapes for different hopping rates and  $b = 100$ . The inset shows one of the line shapes for small applied fields. The lines in (a) and (b) serve as a guide to the eye.

To study the dependence of the MC on the hopping rate, calculations are performed where  $\omega_{\text{hf}}/\omega_{\text{hop}}$  is changed by changing the rate  $r_{\alpha\beta}$  and keeping the branching  $b$ , defined as  $r_{\alpha\beta}/r_{\alpha e}$ , constant. For all calculations we have chosen  $r_{e\alpha} = 10 r_{\alpha\beta}$ . In Fig. 3(a) the MC in large fields,  $\text{MC}_{\infty}$ , is plotted as a function of  $r_{\alpha\beta}$  for three different branching ratios. The curves are obtained by averaging over random configurations of the hyperfine fields. It can be observed that, on increasing the branching ratio, the absolute value of the magnetoconductance also increases, which corresponds to the conclusions of Bobbert *et al.*<sup>5</sup> and Wagemans *et al.*<sup>6</sup> On increasing the hopping rate and leaving the hyperfine-field strengths constant, the MC decreases until it reaches zero. In the fast-hopping regime, the polaron pairs hop so fast that precession around the hyperfine fields is too slow to mix the spin states; thus there is no influence of the hyperfine interactions, resulting in a negligible OMAR.

In Fig. 3(b) the MC is plotted as a function of the applied field for different hopping rates. On increasing the hopping rate not only the magnitude of the magnetoconductance decreases, but also an increase in linewidth is observed. This broadening of the curves is caused by a subtle balance of average polaron pair lifetimes and the amplitude and speed of dephasing, as can be intuitively seen from a simplified classical model. This simplified model, where we consider a single spin

precessing around the sum of an applied field and hyperfine field, yields the following relation for the total amount of mixing in the fast-hopping limit:

$$\Delta_{\text{mix}}(B_{\text{app}}) \propto \frac{\omega_{\text{hf}}^2}{\omega_{\text{hop}}^2} \left( C - \frac{(g\mu_B B_{\text{app}}/\hbar)^2}{\omega_{\text{hop}}^2} \right), \quad (8)$$

where  $C$  is a constant. Two things become apparent from this equation. First, the total amount of mixing becomes small, as can be seen from the prefactor  $\omega_{\text{hf}}^2/\omega_{\text{hop}}^2$ . Second, the linewidth is determined by the ratio between the applied field and the hopping rate; hence, increasing the hopping rate also increases the line-width. Note that in this regime the linewidth is *not* related to the hyperfine-field strength, in sharp contrast to the slow-hopping regime. Conclusively, it is thus not only the hyperfine fields and branching ratio that can influence the linewidths of the MC in OMAR experiments, but also the polaron-pair lifetimes, which is a surprising result from the calculations. Note that this line-shape broadening has not yet been reported in literature, but could be very important for interpreting experimental results. For example, in the recent deuteration experiments performed by Nguyen *et al.*<sup>21</sup> not only the hyperfine-field strength changes on deuteration, but also the ratio  $\omega_{\text{hf}}/\omega_{\text{hop}}$ . The change in linewidth observed in these experiments might thus not be solely caused by the hyperfine interaction strength. Furthermore, in hopping rates between minority and majority charge carriers could also play a role in the large difference in observed linewidths in the sign-change experiments by Bloom *et al.*<sup>22</sup>

Finally, another important feature can be observed in the line shapes depicted in Fig. 3(b). For small applied fields a small positive effect emerges on entering the intermediate-hopping regime, as has recently been discussed by Wagemans *et al.*<sup>23</sup> and Kersten *et al.*<sup>24</sup> To accentuate this effect one of the curves from Fig. 3(b) is depicted in the inset, only zoomed in around the zero applied field. The ultrasmall magnetic-field effect (USMFE) has experimentally been shown to be an intrinsic effect in OMAR,<sup>21</sup> in both unipolar and bipolar devices.<sup>25</sup> The effect is naturally reproduced by the stochastic Liouville equation for the bipolaron model, but also for the e-h pair model discussed in the next section, this without adding any extra terms to the polaron-pair Hamiltonian. The width and size of the effect are determined by the various model parameters and originate from the competition between spin mixing and bipolaron/exciton formation for intermediate-hopping rates, similar to the broadening of the line shapes. In passing we note that adding a small exchange or dipolar interaction to the Hamiltonian will also give rise to the USMFE, as it introduces additional singlet-triplet level crossings for small applied fields.

## IV. ELECTRON-HOLE PAIR MODEL

### A. Basic concepts

A different model for OMAR based on the spin-dependent reactions of polaron pairs is the e-h pair model. The current in an organic semiconductor can be influenced by the recombination rate of polarons. A free hole and electron can form an exciton, which can subsequently decay to the ground state



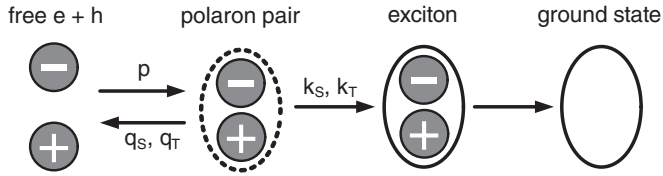


FIG. 4. The e-h pair model as described by Prigodin *et al.*<sup>3</sup> Free electrons and holes form polaron pairs, which can either form an exciton or dissociate. An exciton can decay to the ground state by recombination of the electron and hole. A difference in exciton formation or pair dissociation rate of singlet and triplet e-h pairs yields a MC.

by recombination of the electron and hole, hence removing free charges from the device. Prigodin *et al.*<sup>3</sup> have suggested a model based on the spin-dependent recombination of e-h pairs to explain OMAR, where the recombination rate is susceptible to an applied magnetic field.

A schematic diagram explaining the model is depicted in Fig. 4. In the model it is assumed that before exciton formation, i.e., before spin mixing is frozen by the large exchange interactions, electrons and holes pass through an intermediate state in which they are bound by their Coulomb interaction, but the distance between the pairs is large enough for exchange interactions to be negligible. In this intermediate e-h pair state, the pairs form excitons and subsequently recombine with rates  $k_S$  and  $k_T$  and dissociate with rates  $q_S$  and  $q_T$  for singlet and triplet pairs, respectively. Prigodin *et al.* assume that e-h pairs with a singlet component have a larger exciton formation rate  $k_S$  and thus a larger recombination probability. However, Xu and Hu conjecture that the magnetoresistance is not caused by a difference in recombination rate of singlet and triplet e-h pairs, but by a difference in dissociation rate due to the more ionic nature of the singlet e-h pairs.<sup>26</sup> As the resulting influence on the MC for both mechanisms is almost identical, we will focus on the model of Prigodin *et al.*, where we assume that there is a smaller recombination rate of triplet than singlet e-h pairs. Note that this is in sharp contrast to what is concluded by Kersten *et al.*,<sup>27</sup> where the triplet e-h pairs have the largest recombination rate. As it does not lie within the scope of this paper to justify these assumptions we use the model of Prigodin *et al.* in the calculations.

Just as in the bipolaron model, the hyperfine fields experienced by the polarons in the pair mix the singlet and triplet spin states. On applying a magnetic field, the mixing by the hyperfine fields is suppressed. If one now assumes that singlet pairs have a larger recombination rate than triplet pairs, increasing the magnetic field leads to less pair states being mixed with the singlet state and thus less recombination, ordinarily resulting in a larger current. However, not only recombination but also space charge plays an important role in the current through an organic light-emitting diode (OLED). Therefore, there is a different relation between the recombination probability and the current for different operating regimes. In this paper we will for simplicity restrict the calculations to the space-charge-limited transport regime; however, extending the calculations to other regimes is straightforward.

## B. Electron-hole recombination: Density-matrix calculations

The current through an OLED operated in the space-charge-limited transport regime is given by<sup>3</sup>

$$J = \frac{3\epsilon}{4} \sqrt{\frac{2\pi\mu_e\mu_h(\mu_e + \mu_h)}{\mu_{\text{rec}}}} \left(\frac{V^2}{d^3}\right), \quad (9)$$

where  $\mu_e$  and  $\mu_h$  are the electron and hole mobilities, respectively,  $\mu_{\text{rec}}$  the so-called recombination mobility,  $\epsilon$  is the dielectric constant of the material,  $d$  is the thickness of the device, and  $V$  is the applied voltage. Note that the relation is valid for only a trap-free bipolar device and two ohmic contacts. Prigodin *et al.* argue that a magnetic field changes the recombination mobility of Coulombically bound e-h pairs. The recombination mobility is given by<sup>28</sup>

$$\mu_{\text{rec}} = \frac{\epsilon a P_{\text{rec}}}{2e}, \quad (10)$$

where  $a$  is given by the Langevin equation<sup>3</sup> and  $P_{\text{rec}}$  is the probability that after formation an e-h pair recombines instead of dissociates. To calculate the recombination probability we consider an e-h pair on two neighboring localized sites  $\alpha$  and  $\beta$ . The spin part of the polaron-pair Hamiltonian is given by Eq. (5). On creation of the polaron pair again it is assumed that the spins show no correlation; hence the density matrix at  $t = 0$  is proportional to the identity matrix. The time evolution of the density matrix of an ensemble of e-h pairs created at  $t = 0$  is given by

$$\begin{aligned} \frac{\partial \rho}{\partial t} = & -\frac{i}{\hbar}[H, \rho] - \frac{1}{2}(q_S + k_S)\{\Lambda_S, \rho\} \\ & - \frac{1}{2}(q_T + k_T)\{\Lambda_T, \rho\}. \end{aligned} \quad (11)$$

$\rho(t)$  can now be calculated by solving Eq. (11). The recombination probability of an e-h pair is given by

$$P_{\text{rec}} = \int_{t=0}^{\infty} \frac{k_S \rho_S(t) + k_T \rho_T(t)}{(k_S + q_S)\rho_S(t) + (k_T + q_T)\rho_T(t)} dt, \quad (12)$$

where  $\rho_S(t)$  and  $\rho_T(t)$  are, respectively, the singlet and triplet densities of the ensemble, which are just the diagonal elements of  $\rho$  in a basis of the eigenstates of the total spin operator  $\hat{S}^2$ . Solving the set of coupled differential equations and integrating the results is, however, a numerically demanding task. A more convenient approach to this problem is given by Hansen and Pedersen,<sup>29</sup> who consider a system of interacting radical pairs that are continuously being created. The steady-state solution of the system is used to calculate the recombination probability of a single radical pair. This steady-state approach yields results identical to the ones obtained by integrating the time-dependent solutions of the system, as long as there is no spin-dependent interaction between the individual pairs.

Equation (11) is adapted by adding a source term, resulting in the following steady-state relation:

$$\begin{aligned} 0 = & -\frac{i}{\hbar}[H, \rho] - \frac{1}{2}(q_S + k_S)\{\Lambda_S, \rho\} \\ & - \frac{1}{2}(q_T + k_T)\{\Lambda_T, \rho\} + \frac{1}{4}p\Gamma, \end{aligned} \quad (13)$$

where  $p$  is the e-h pair formation rate and  $\Gamma$  is the identity matrix. Note that the resulting equation has exactly the same

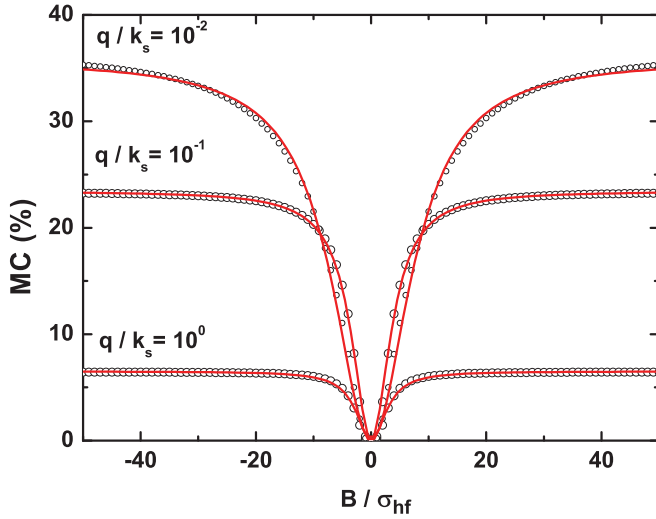


FIG. 5. (Color online) MC as a function of the applied field for the e-h pair model for three values of  $q/k_S$  while  $q_S = q_T = q$  and  $k_T = 0$ . The dots are the results from the calculations while the lines are fits of the data with Lorentzians.

form as the stochastic Liouville equation from Eq. (4). After solving Eq. (13),  $P_{\text{rec}}$  is calculated with

$$P_{\text{rec}} = \frac{k_S \rho_S + k_T \rho_T}{(k_S + q_S) \rho_S + (k_T + q_T) \rho_T}. \quad (14)$$

Note that the recombination probability of the e-h pair is independent of the formation rate  $p$ .  $P_{\text{rec}}$  can now be used to calculate the recombination mobility with Eq. (10). By entering the recombination mobility in Eq. (9) the current in the space-charge-limited transport regime is calculated.

Finally, the MC is obtained by evaluating Eq. (7). By following this procedure MC line shapes can be calculated. In the next sections we will show how the model parameters of the e-h pair model change the MC in OLEDs. Furthermore, an application of this density-matrix approach is illustrated by investigating the influence of a difference in  $g$  factors of the electron and hole.

### C. Magnetoconductance and line shapes

For the e-h pair model of Prigodin *et al.*<sup>3</sup> no theoretical MC line shapes have ever been reported in the literature. Therefore some line shapes are calculated and analyzed here. For the calculations we assumed  $q_S = q_T = q$ , i.e., the triplet and singlet pairs have equal dissociation rates, and  $k_T = 0$ , meaning that triplet pairs cannot recombine. Furthermore, calculations are performed in the slow-hopping limit, so  $\omega_{\text{hf}}/\omega_{\text{hop}} \gg 1$ . The resulting line shapes are depicted in Fig. 5. The first thing to notice is that the MC due to e-h pair recombination is positive, i.e., an applied field increases the current. Second, the line shapes can be fitted reasonably well with a Lorentzian, which is one of the two experimentally observed OMAR line shapes.<sup>30</sup> Also, the Lorentzian has previously been obtained from simple calculations on the MC due to suppression of the hyperfine fields by an applied field.<sup>31</sup> One of the reasons that the obtained line shapes are not exactly Lorentzian is the averaging over the random hyperfine fields, as adding the Lorentzians from the single hyperfine-field strengths yields a

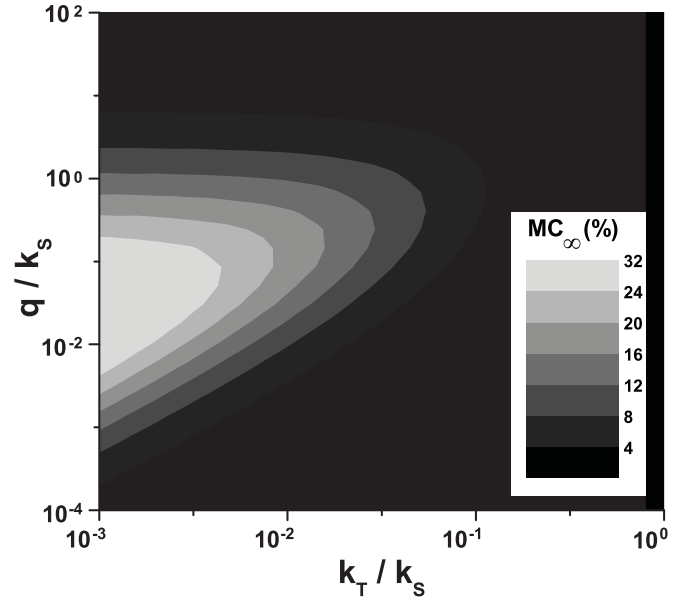


FIG. 6. Contour plot of the MC as a function of  $q/k_S$  and  $k_T/k_S$  in the e-h pair model.

slightly broadened curve at small fields. A final observation that can be made is that the line shapes are altered by model parameters. On increasing the ratio  $q/k_S$  a broadening of the line-shape is observed, resulting in a larger deviation from the Lorentzian line shape. From this observation we can conclude that not only the hyperfine-field strength and polaron-pair lifetime, but also the rates influence the line shape. We would like to note that the dependence of the line shapes on the model parameters in the e-h pair model is less pronounced as compared with the bipolaron model, as in the latter non-Lorentzian line shapes can be produced due to strong blocking of crucial percolation paths,<sup>6</sup> whereas in the e-h pair model the line shapes always more closely resemble Lorentzians.

To further investigate the influence of the model parameters in the e-h pair model, a contour plot of  $MC_{\infty}$  is shown in Fig. 6 for different values of the ratios  $q/k_S$  and  $k_T/k_S$ . What can be observed is that, irrespective of the value of  $q/k_S$ , increasing the triplet recombination rate  $k_T$  leads to a smaller MC; thus the larger the difference between the triplet and singlet recombination rates, the larger the MC. When  $k_T/k_S = 1$ , no MC is observed as singlets and triplets recombine with the same rate.

On increasing  $q/k_S$  we see in Fig. 6 that at first the MC increases, but starts decreasing after reaching a maximum. This can be qualitatively explained as follows: When  $q \gg k_S$ ,  $\rho_S$  and  $\rho_T$  are not changed by the magnetic field as the spin-dependent recombination step becomes small compared with spin-independent dissociation. When  $q \ll k_T$ , pairs with only a triplet component will also recombine; hence suppression of spin mixing by the applied magnetic field does not influence the recombination probability of the polaron pairs. This means that for moderate values of  $q$  with respect to  $k_S$  and  $k_T$  the maximum MC can be observed.

To sum up our findings we can conclude that calculations on the MC due to e-h pair formation yield Lorentzian-like

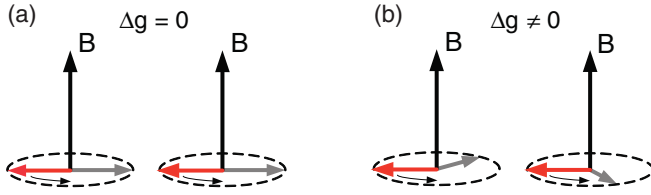


FIG. 7. (Color online) Classical representation of spin mixing due to the  $\Delta g$  mechanism. (a) The e-h pair starting in the  $|T_0\rangle$  state remains in the  $|T_0\rangle$  state as both spins precess in phase around the applied field. (b) The  $|T_0\rangle$  state is mixed with the  $|S_0\rangle$  state due to a difference in precession frequency.

line shapes. Linewidths are affected by both hyperfine-field strengths and recombination/dissociation rates, while the size of the effect is mostly determined by the latter. We note that in real devices there is a distribution of hopping rates due to the disordered nature of the organic semiconductors. Averaging over these different hopping rates could result in more realistic line shapes, but is a numerically demanding task.

#### D. $\Delta g$ mixing

In the e-h pair and bipolaron model, a spin-pair Hamiltonian is used where the  $g$  factors of both the charge carriers are identical. However, this is not necessarily the case for realistic devices, where the  $g$  factors of the electrons and holes might differ. Furthermore, polarons with the same charge might also have different  $g$  factors due to a slightly different chemical environment.<sup>32</sup> In the literature it is suggested that this difference in  $g$  factors leads to a magnetic-field-dependent mixing of the  $|S_0\rangle$  and  $|T_0\rangle$  states in large applied fields. It is argued that this  $\Delta g$  mechanism yields a  $\sqrt{B}$  magnetic-field dependence of the recombination rate for radical pairs,<sup>17</sup> but it has never been explicitly shown that this dependence holds for the different OMAR models as assumed, for example, by Wang *et al.*<sup>7</sup> Therefore, we will study the MC in the e-h pair model with a small difference in  $g$  factors of the electron and hole using the stochastic Liouville equation.

The  $|S_0\rangle$  and  $|T_0\rangle$  states can classically be thought of as the states with the spins perpendicular to the applied magnetic field, where in the  $|T_0\rangle$  state the spins precess in phase around the magnetic field, while in the  $|S_0\rangle$  state the spins precess out of phase around the field. A difference in  $g$  factors results in a difference in precession frequency, hence the  $|S_0\rangle$  and  $|T_0\rangle$  states are mixed by the applied field. A schematical drawing illustrating this dephasing is shown in Fig. 7. Note that a small exchange interaction or dipole coupling is necessary to observe the  $\Delta g$  mechanism, because the  $|T_0\rangle$  and  $|S_0\rangle$  states need to be split in energy at zero field, otherwise the  $|S_0\rangle$  and  $|T_0\rangle$  states are already fully mixed by the hyperfine interactions; hence an increased mixing due to the  $\Delta g$  mechanism would not be observable. The following term has to be added to the polaron-pair Hamiltonian in Eq. (5):

$$H_{\text{ex}} = J\left(\frac{1}{2} + 2\vec{S}_\alpha \cdot \vec{S}_\beta / \hbar^2\right), \quad (15)$$

where  $J$  is the exchange interaction strength, which depends on the overlap of the wave functions of the electron and hole.

To illustrate how a MC line shape is influenced by the  $\Delta g$  mechanism, calculations are performed in the e-h pair

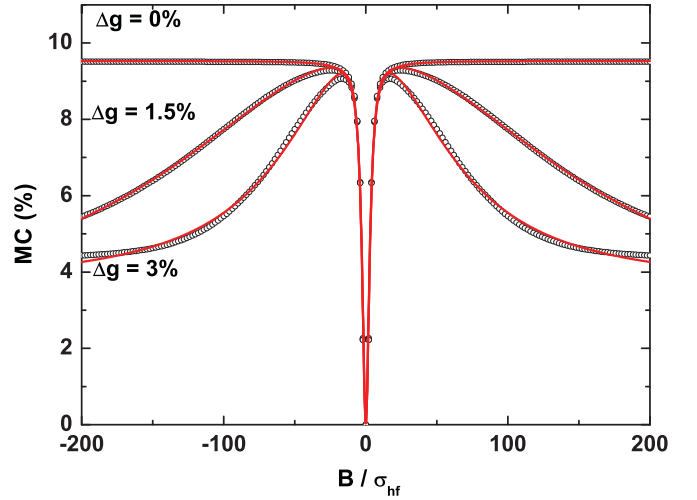


FIG. 8. (Color online) MC line shapes due to  $\Delta g$  mixing in the e-h pair model in the slow-hopping regime. The lines are fits to double Lorentzians. The chosen model parameters are  $k_T/k_S = 0$ ,  $q/k_S = 1$ , and  $J = 0.3 \mu_B \sigma_{\text{hf}}$ .

model, where a small difference in  $g$  factors of the electron and hole is introduced. The resulting line shapes for three differences in  $g$  factors are shown in Fig. 8. The calculated line shapes show a sharp increase around zero field due to the suppression of the hyperfine mixing of the  $|T_1\rangle$  and  $|T_{-1}\rangle$  states with the  $|S_0\rangle$  and  $|T_0\rangle$  states. On increasing the magnetic field further a decrease in magnetoconductance is observed due to increasing  $\Delta g$ -mixing. The decrease of the MC resembles a Lorentzian-like line shape, as the total line shapes are fitted reasonably well with two Lorentzians. At large fields the MC is saturated, because the  $|S_0\rangle$  and  $|T_0\rangle$  states are completely mixed. The high field linewidth is determined by the difference in  $g$  factors and the exchange interaction strength, while the magnitude of the effect is determined by the relative size of the exchange and hyperfine interactions.

The most important conclusions on the  $\Delta g$  mechanism that can be drawn from the calculations are (i)  $\Delta g$  gives a Lorentzian-like line shape in the e-h pair model, different from the  $\sqrt{B}$  dependence proposed and reported in the literature.<sup>7</sup> This discrepancy is caused by the fact that in the literature it is assumed that the exchange energy is negligible compared with the  $\Delta g$  mixing, while the effect is most pronounced when both interactions are of equal magnitude. Furthermore, random encounter processes are taken into account as the derivation is performed for free radicals in solution. This means that although many successful models for magnetic-field-dependent reactions have been introduced in spin chemistry,<sup>17</sup> one has to be careful with naively applying them to OMAR. (ii) The linewidth is solely determined by the exchange interaction and the difference between the  $g$  factors. (iii) The magnitude of the  $\Delta g$  mechanism is determined by the ratio of the hyperfine and the exchange interactions. (iv) The  $\Delta g$  mechanism yields an opposite effect to the suppression of the hyperfine fields, in contradiction to the suggestions in the literature.<sup>7</sup> (v) Because the exchange interaction has to be of the order of the hyperfine interaction strength for the  $\Delta g$  mechanism to be significant, the difference in  $g$  factors needs to be large ( $\approx 1\%$ ) for the effect to be visible in experimentally

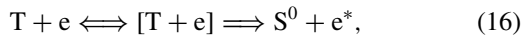
feasible magnetic fields ( $<1$  T). We therefore conjecture that high-field effects in the current in OLEDs with linewidths of  $\approx 100$  mT cannot be explained by a difference in  $g$  factors between the electron and hole in a pair.

## V. TRIPLET-CHARGE REACTIONS

### A. Basic concepts

Johnson *et al.*<sup>33</sup> have shown that triplet exciton reactions in anthracene single crystals can give rise to a magnetic-field effect on the delayed photoluminescence in these crystals. In the literature the high-field effect on the photocurrent, and even regular OMAR, is sometimes explained by these reactions of triplet excitons.<sup>34,35</sup> However, most of the calculations on triplet reactions in the literature are focused on single crystals.<sup>13,33,36</sup> We will use the stochastic Liouville equation to study the magnetic-field-dependence of triplet reactions in *disordered* organic semiconductors. We will discuss the two most important magnetic-field-dependent reactions involving triplet excitons, namely triplet-triplet (T-T) annihilation and triplet-charge reactions.

Triplet excitons, which in general have a far longer lifetime in organic semiconductors than singlet excitons,<sup>37,38</sup> can react with trapped charges in the following manner:<sup>39</sup>



where  $T$  is the triplet exciton,  $e$  and  $e^*$  are a trapped and a free electron, respectively, and  $S^0$  is the singlet ground state of a molecule. Note that the electron could also be a hole, as the reaction of a hole with a triplet is identical. Therefore, we refer to an electron or a hole as a doublet (D), since both have a total spin of  $1/2$ . The reactions of triplet excitons with trapped charges can have a severe influence on the current of an OLED, as the mobility of the charges can be enhanced, especially under photoexcitation. In the literature the term photoenhanced current is introduced for this effect.<sup>40</sup>

Because the total spin of the triplet-doublet pair (T-D pair) after the reaction is  $1/2$ , the total spin of the two particles before the reaction is required to also be  $1/2$  due to spin conservation. Because the triplet is a spin-1 particle and the trapped charge carrier a spin- $1/2$  particle, the total spin of the pair can be either  $3/2$  (quartet  $|Q\rangle$ ) or  $1/2$  (doublet  $|D\rangle$ ). It is thus required that the two-particle wave function has a doublet character in order to react. Note that we refer to the doublet spin state of the T-D pair with the ket notation, i.e.,  $|D\rangle$ , while we refer to the doublet as the individual electron or hole particle with D. As the reaction in Eq. (16) annihilates triplet excitons, we will call this process T-D quenching.

### B. Density matrix implementation

To perform calculations on T-D quenching, we use a model that is schematically depicted in Fig. 9. Triplets and doublets form T-D pairs with a rate  $k_1$  and dissociate with a rate  $k_{-1}$ . The two-particle T-D pair wave function will evolve in time according to the corresponding Hamiltonian and during this time the quartet and doublet states can mix. The triplet in a pair that has a doublet character will relax to the ground state with a rate  $k_2$  on detrapping the charge carrier by

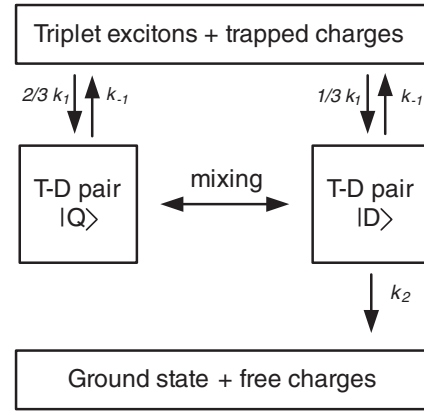


FIG. 9. Schematic diagram of triplet-charge reactions. Only pairs in the doublet state can react, where the triplet exciton will transfer its energy to detrapp the charge. The mixing rate is magnetic-field dependent, yielding a magnetic-field-dependent T-D reaction rate.

transferring its energy. To model T-D quenching the following spin Hamiltonian is used:

$$\begin{aligned} H &= H_{Z,T} + H_{Z,D} + H_{hf,T} + H_{hf,D} + H_{zfs,T}, \\ H_{Z,i} &= \frac{g\mu_B}{\hbar} \vec{B}_{app} \cdot \vec{S}_i, \\ H_{hf,i} &= \frac{g\mu_B}{\hbar} \vec{B}_{hf,i} \cdot \vec{S}_i, \\ H_{zfs,T} &= \frac{D_{zfs}}{\hbar^2} S_{T,z}^2 + \frac{E_{zfs}}{\hbar^2} (S_{T,x}^2 - S_{T,y}^2), \end{aligned} \quad (17)$$

where  $\vec{S}_T$  and  $\vec{S}_D$  are the spin operators for the triplet and doublet particle respectively,  $S_{T,x}$ ,  $S_{T,y}$ , and  $S_{T,z}$  are the Pauli spin matrices for the triplet exciton,  $D_{zfs}$  and  $E_{zfs}$  are the zero-field splitting (zfs) parameters of the triplet exciton, and  $\vec{B}_{hf,T}$  and  $\vec{B}_{hf,D}$  are the hyperfine fields experienced by the triplet and doublet, respectively. The zfs of an exciton is caused by spin-spin interactions, for example, a dipole coupling, between the hole and the electron, thus splitting the energy of the  $|T_1\rangle$ ,  $|T_0\rangle$  and  $|T_{-1}\rangle$  states. Finally, it has to be noted that the Hamiltonian is valid only in a coordinate system of the molecule where the  $x$ ,  $y$ , and  $z$  axes coincide with the principal zfs axes.

To calculate the magnetic-field dependence of T-D quenching, the following stochastic Liouville equation has to be solved:

$$\begin{aligned} 0 &= -\frac{i}{\hbar} [H, \rho] - \frac{1}{2} (k_{-1} + k_2) \{\Lambda_D, \rho\} \\ &\quad - \frac{1}{2} k_{-1} \{\Lambda_Q, \rho\} + \frac{1}{6} k_1 \Gamma, \end{aligned} \quad (18)$$

where  $\Lambda_D$  and  $\Lambda_Q$  are projection operators on the doublet and quartet spin states. Note that again the steady-state approach is used to simplify calculations. After solving Eq. (18), the T-D quenching probability  $P_q$  can be calculated as follows:

$$P_q = \frac{k_2 \rho_D}{(k_2 + k_{-1}) \rho_D + k_{-1} \rho_Q}, \quad (19)$$

where  $\rho_D$  and  $\rho_Q$  are, respectively, the doublet and quartet densities of the ensemble, which can be easily obtained from the density matrix.  $P_q$  is the probability that, on forming a T-D pair, the triplet is quenched and the charge carrier is detrapped.



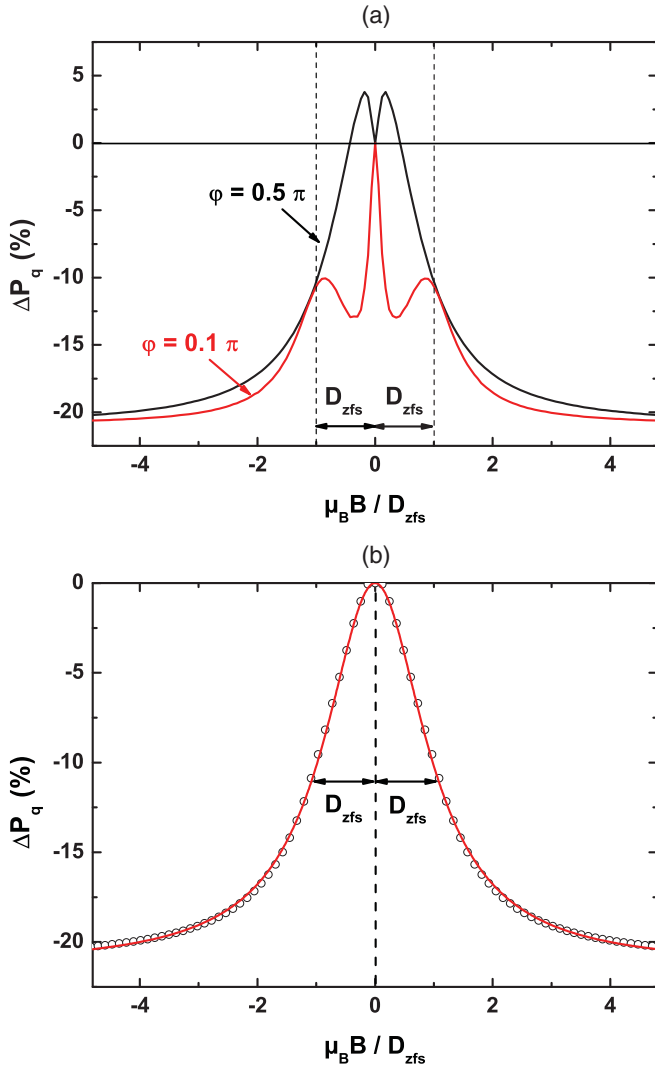


FIG. 10. (Color online) (a) T-D line shapes for two specific orientations of the zfs principal axis with respect to the magnetic field. (b) T-D line shape after averaging over all possible orientations of a molecule in an applied field. The line is a fit with a Lorentzian. Calculations for (a) and (b) are performed for  $D_{zfs} = 10\mu_B\sigma_{hf}$  and  $k_2 = 10k_{-1}$

When  $P_q$  is small, i.e.,  $P_q \ll 1$ , the triplets and doublets do not react, while a large  $P_q$ , i.e.,  $P_q \approx 1$ , indicates a large reaction rate. The relative change in the reaction rate on applying a magnetic field is defined as

$$\Delta P_q(B) = \frac{P_q(B) - P_q(0)}{P_q(0)} 100 \%. \quad (20)$$

The influence of triplet-charge reactions on the current can be both positive (by detrapping of charges or reduced site blocking by triplet excitons<sup>41</sup>) and negative (by quenching of excitons), depending on the operating conditions of the device. Therefore,  $\Delta P_q(B)$  will be the main parameter of interest in the calculations. A macroscopic device model is required to investigate the final influence of  $\Delta P_q(B)$  on the current, which is beyond the scope of this paper.

### C. Calculations

In Figs. 10(a) and 10(b) calculations are shown of the triplet quenching rate as a function of the applied magnetic field. The zfs interaction strengths are chosen to be  $D_{zfs} = 10\mu_B\sigma_{hf}$ , as in general the zero-field interaction is stronger than the hyperfine interaction.<sup>42</sup> To reduce computation time,  $E_{zfs}$  is set to zero, so there is only one principal axis, hence a larger symmetry in the system. Calculations are performed in the slow-hopping regime, i.e., in the regime where mixing is faster than the rates in the Liouville equation.

In Fig. 10(a) the magnetic-field dependence of the quenching rate is plotted for two angles  $\phi$  between the magnetic field and the principal zfs axis, which is the  $z$  axis in the molecular frame of reference. Numerical averaging is performed over random orientations of the hyperfine fields. In the graph a sharp feature can be observed for small applied fields, which can be attributed to the hyperfine interactions. At larger fields, around  $D_{zfs}$ , peaks can also be observed for specific orientations, which are due to level crossings of the doublet and quartet states.

For the devices studied in this paper, the molecules have a random orientation in the sample, i.e., the medium is disordered. Note that in the literature no quantitative calculations have been performed on the line shapes due to T-D quenching in disordered media; only calculations on single crystals have been reported.<sup>36</sup> To calculate the quenching rate for these disordered media; a numerical integration is performed over the different orientations of the triplet host molecule in the applied field. A typical result of such a calculation is plotted in Fig. 10(b). The quenching rate is now a monotonous decreasing function of the magnetic field and can be fitted remarkably well with a Lorentzian, although the fit is not perfect, which could be expected as the curves in Fig. 10(a) are no Lorentzians either. Important to notice is that the influence of the hyperfine fields is canceled out by the integration over the different angles, hence no features are visible for small applied fields. *This means that the width is fully determined by the zfs strength and not by the hyperfine interactions.*

To see how the T-D pair lifetime influences the quenching probability, calculations are performed where the recombination/dissociation ratio  $k_2/k_{-1}$  is kept constant. Again the pair creation rate  $k_1$  is not of interest for  $P_q$ , since the pairs do not interact with each other. The results of the calculations are shown in Fig. 11. Here the T-D quenching probability in large fields is plotted as a function of the dissociation rate. What can be observed is that, for small dissociation rates, hence also small recombination rates, the magnetic-field effect is large. On decreasing the pair lifetime, i.e., increasing  $k_{-1}$ , first mixing by the hyperfine fields is lost, as the precession period of the spins around the field becomes larger than the pair lifetime. This loss of hyperfine mixing results in the bump, i.e., a small decrease followed by a small increase, observed in the graph. On further decreasing the pair lifetime the zfs interactions also become too weak to mix the spin states; hence the magnetic-field effect is totally quenched. This second result is identical to what we see on decreasing polaron-pair lifetimes in the polaron-pair models, where the magnetic-field effect vanishes for very small lifetimes, as can be seen in Fig. 3(a).

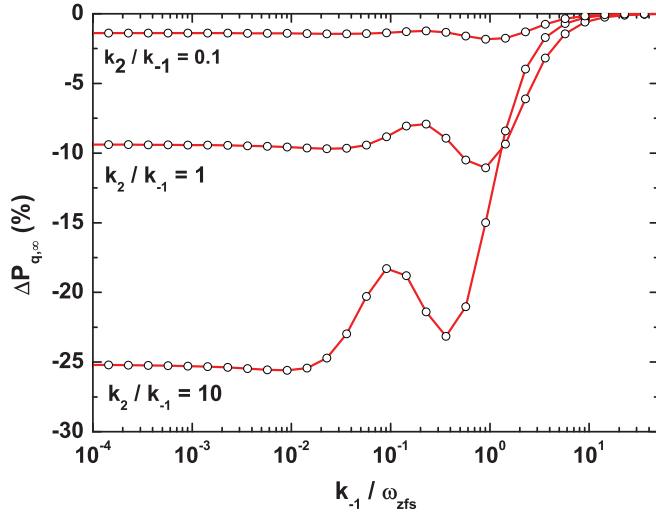
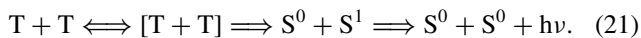


FIG. 11. (Color online) Influence of the T-D pair lifetime on the reaction probability in large applied fields. Increasing the hopping rates results in a quenching of the magnetic-field effect, as mixing by the hyperfine and zfs reactions plays no role for very small pair lifetimes.

To summarize our findings of this section, we have successfully calculated line shapes due to T-D quenching in a disordered semiconductor, taking the zfs and hyperfine interactions into account. We have seen that an applied magnetic field decreases the reaction rate between triplet excitons and charge carriers. An important result is the Lorentzian-like line shape with a linewidth determined by the zfs strength, which is obtained after averaging over all possible angles between the magnetic field and the molecule hosting the triplet exciton. The influence of the hyperfine interactions on the line shapes is effectively removed by this averaging procedure. Finally, the effect of the lifetime of the T-D pair on the reaction rate is investigated. When the lifetime of the pair is sufficiently small, the magnetic-field effect on the reactions is effectively quenched, comparable to the polaron-pair models. The influence of the pair lifetime is more complicated in the T-D case, as both the hyperfine and the zfs interactions have different characteristic mixing times.

## VI. TRIPLET-TRIPLET ANNIHILATION

Another magnetic-field-dependent reaction of triplet excitons in organic semiconductors is the mutual annihilation of triplet excitons. When two triplet excitons react, they can annihilate on creation of a ground-state singlet and an excited singlet, which will quickly relax to the ground state on emitting a photon:<sup>33</sup>



The energy of both triplets is transferred to the excited singlet exciton state. As triplet excitons can influence the mobility of charge carriers,<sup>44</sup> a magnetic-field dependence of the mutual annihilation of triplet excitons could yield a magnetic-field effect on the current, as the triplet density becomes sensitive to an applied magnetic field.

Spin conservation rules require that a T-T pair needs to have zero total spin to annihilate, i.e., the T-T pair needs to

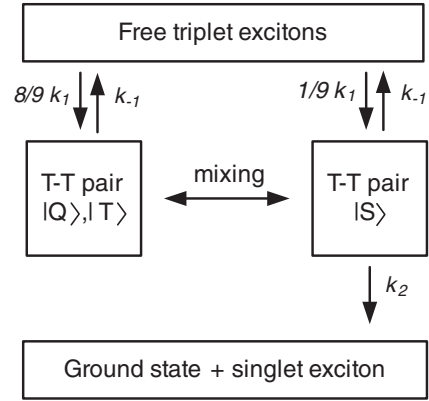


FIG. 12. Schematic diagram of the mutual annihilation of triplet excitons. Only singlet pairs react, resulting in an annihilated exciton and an excited singlet. The mixing rate between the singlet, triplet, and quintet spin states is magnetic-field-dependent, yielding a magnetic-field-dependent T-D reaction rate.

have a singlet character. The magnetic-field effect on T-T annihilation is very similar to the T-D quenching effect, and a schematic diagram of the T-T annihilation process is shown in Fig. 12. T-T pairs are formed with a rate  $k_1$ , and the spin state of the pair evolves in time according to the pair Hamiltonian. When a T-T pair has a singlet character, it will annihilate with a rate  $k_2$ . Pairs also dissociate back into free triplets with a rate  $k_{-1}$ , irrespective of the spin state of the pair. Due to the many similarities with T-D quenching, like the interactions responsible for mixing, we will show only a limited amount of calculations on T-T annihilation. More calculations on this reaction have been reported in the literature.<sup>13,45</sup>

The typical Hamiltonian of a molecular T-T pair is

$$H = H_{Z,\alpha} + H_{Z,\beta} + H_{\text{hf},\alpha} + H_{\text{hf},\beta} + H_{\text{zfs},\alpha} + H_{\text{zfs},\beta}, \quad (22)$$

where the Zeeman, hyperfine, and zfs terms are identical to the ones in Eq. (17). To calculate the magnetic-field dependence of T-T annihilation the following stochastic Liouville equation is used:

$$\frac{\partial \rho}{\partial t} = -\frac{i}{\hbar}[H, \rho] - \frac{1}{2}(k_{-1} + k_2)\{\Lambda_S, \rho\} - \frac{1}{2}k_{-1}\{\Lambda_{T,Q}, \rho\} + \frac{1}{9}k_1\Gamma, \quad (23)$$

where  $\Lambda_S$  and  $\Lambda_{T,Q}$  are projection operators on the singlet and triplet-quintet spin states. By solving Eq. (23) for steady-state conditions, the probability that a formed T-T pair annihilates can be calculated with

$$P_A = \frac{k_2 \rho_S}{(k_2 + k_{-1})\rho_S + k_{-1}\rho_{T,Q}}, \quad (24)$$

where  $\rho_S$  and  $\rho_{T,Q}$  are respectively the singlet and triplet-quintet densities. As we investigate the magnetic-field effect in disordered systems, we need to average over every possible mutual orientation of the zfs principal axes of the two excitons. In the literature, averaging over different orientations has been performed using different methods;<sup>43,45</sup> however, the perturbation theory used in both articles is valid for only a limited range of model parameters. In Fig. 13 we present

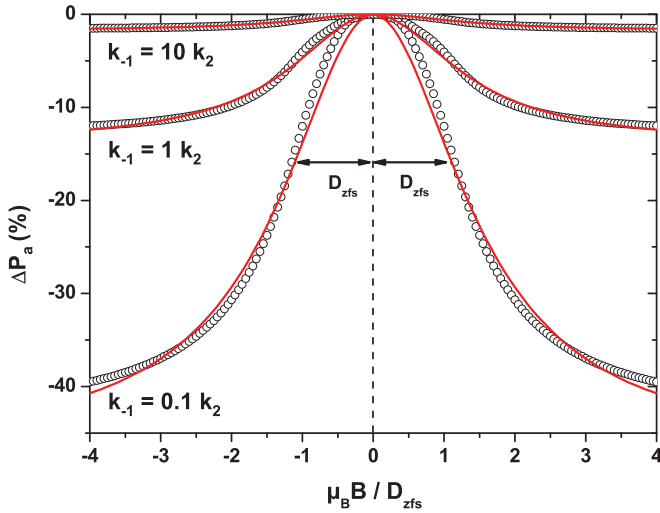


FIG. 13. (Color online) T-T annihilation line shapes after averaging over random zfs principal axes and hyperfine fields. The lines are fits with Lorentzians while the dots are the results from the density-matrix calculations. In the calculations  $D_{zfs} = 10\mu_B\sigma_{hf}$  and  $k_1 = k_2$ .

the resulting line shapes for T-T annihilation for disordered organic semiconductors. Averaging has been performed over random configurations of the hyperfine fields and zfs principal axes. In the calculations  $D_{zfs} = 10\mu_B\sigma_{hf}$  and  $k_1 = k_2$  while the line shapes for different  $k_{-1}$  are plotted.

What can be observed from the calculations in Fig. 13 is that the resulting line shapes for T-T annihilation in organic semiconductors cannot be fitted as accurately with a Lorentzian as the ones for T-D quenching. However, as for T-D quenching, the line shape is fully determined by the zfs interactions while the hyperfine fields are canceled out. The calculations support the claims made by Avakian *et al.*<sup>43</sup> and Mezyk *et al.*<sup>46</sup> that T-T annihilation for randomly oriented molecules results in a monotonous decrease of the T-T annihilation rate.

## VII. OUTLOOK

We have shown in this paper that with a single mathematical framework, namely the stochastic Liouville equation, it is possible to perform calculations on different spin-dependent reactions in organic semiconductors. Besides the reactions discussed in this article, there are many more mechanisms that could be investigated by only slightly altering the stochastic Liouville equation. For example, one could model the spin-dependent generation of a photocurrent by using this method. Furthermore, there are possibilities to further improve the method in a way to represent realistic devices more accurately. One could, for example, take diffusion of the particles in a pair into account in the stochastic Liouville equation, as has been done by Suna.<sup>47</sup> Also, integrating over a distribution of hopping rates that is realistic for the studied devices could provide more insight into the physics governing these devices. Another interesting approach is to combine the Liouville equation with the device model as presented by Bloom *et al.*,<sup>48</sup> making it possible to study not only the microscopic properties but at the same time also the influence on the macroscopic properties of

the system under investigation. This can be done by adding the magnetic-field-dependent recombination probability  $P_{rec}(B)$  to the transport simulations used by Bloom *et al.*

Finally, combining the results from calculations and measurements could prove useful in interpreting experimental data, especially where not only low-field (<20 mT) but also high-field effects are visible. By studying parameters like the linewidth and sign of the effects as a function of operating conditions of a device and comparing them with the microscopic calculations, further insight into charge transport in organic semiconductors can be obtained.

## VIII. CONCLUSIONS

The stochastic Liouville equation enabled us to perform calculations on the two-site bipolaron model for general polaron-pair lifetimes. An important observation is that a decrease in polaron-pair lifetime not only quenches the magnitude of the MC, but that the polaron-pair lifetime also strongly influences linewidths of the MC.

Line shapes for the e-h pair model have been calculated. The magnetic-field dependence of e-h pair recombination yields mainly Lorentzian line shapes. The influence of the different model parameters has been investigated. Also the influence of a difference in  $g$  factors between the electron and hole in a pair has been studied, yielding a contribution to the MC in large applied fields that is *opposite* to the contributions due to suppression of the hyperfine fields. The  $\Delta g$  mechanism yields a Lorentzian-like line shape, which is different from the  $\sqrt{B}$  dependence reported in the literature.

Finally, the magnetic-field dependence of the reactions involving triplet excitons has been calculated. The detrapping rate of charges by triplet excitons has been examined in the case of disorder media, resulting in Lorentzian-like line shapes that are monotonically decreasing on increasing the applied field. Linewidths are fully determined by the zfs strength while the influence of the hyperfine fields is washed out. A similar conclusion can be drawn for the mutual annihilation rate of triplet excitons in an external field, confirming claims by Avakian *et al.*<sup>43</sup> and Mezyk *et al.*<sup>46</sup>

More important, we have shown that the stochastic Liouville equation is a powerful and versatile tool to perform calculations on all the different models for organic magnetoresistance referred to in the literature. By adapting both the stochastic Liouville equation as the system Hamiltonian we were able to calculate the magnetic-field dependence of the various spin-dependent reactions. By combining the stochastic Liouville equation with experimental data, more insight into which particular spin-dependent reactions dominate magnetic-field effects on charge transport in organic semiconductors could in the future be obtained.

## ACKNOWLEDGMENTS

This work was supported by the Dutch Technology Foundation STW via the NWO VICI-grant Spin Engineering in Molecular Devices (Project No. 06628) and was part of the research programme of the Foundation for Fundamental Research on Matter (FOM), which is part of the Netherlands Organisation for Scientific Research (NWO).

\*a.j.schellekens@tue.nl

- <sup>1</sup>T. L. Francis, Ö. Mermer, G. Veeraraghavan, and M. Wohlgenannt, *New J. Phys.* **6**, 185 (2004).
- <sup>2</sup>J. Kalinowski, J. Szymkowski, and W. Stampor, *Chem. Phys. Lett.* **378**, 380 (2003).
- <sup>3</sup>V. N. Prigodin, J. D. Bergeson, D. M. Lincoln, and A. J. Epstein, *Synth. Met.* **156**, 757 (2006).
- <sup>4</sup>P. Desai, P. Shakya, T. Kreouzis, W. P. Gillin, N. A. Morley, and M. R. J. Gibbs, *Phys. Rev. B* **75**, 094423 (2007).
- <sup>5</sup>P. A. Bobbert, T. D. Nguyen, F. W. A. van Oost, B. Koopmans, and M. Wohlgenannt, *Phys. Rev. Lett.* **99**, 216801 (2007).
- <sup>6</sup>W. Wagemans, F. L. Bloom, P. A. Bobbert, M. Wohlgenannt, and B. Koopmans, *J. Appl. Phys.* **103**, 07F303 (2008).
- <sup>7</sup>F. J. Wang, H. Bässler, and Z. Valy Vardeny, *Phys. Rev. Lett.* **101**, 236805 (2008).
- <sup>8</sup>S. Majumdar, H. S. Majumdar, H. Aarnio, D. Vanderzande, R. Laiho, and R. Österbacka, *Phys. Rev. B* **79**, 201202 (2009).
- <sup>9</sup>Z. Xu, Y. Wu, and B. Hu, *Appl. Phys. Lett.* **89**, 131116 (2006).
- <sup>10</sup>P. Desai, P. Shakya, T. Kreouzis, and W. P. Gillin, *Phys. Rev. B* **76**, 235202 (2007).
- <sup>11</sup>Y. Goto, T. Noguchi, U. Takeuchi, K. Hatabayashi, Y. Hirose, T. Uchida, T. Sasaki, T. Hasegawa, and T. Shimada, *Organic Electronics* **11**, 1212 (2010).
- <sup>12</sup>R. Haberkorn, *Chem. Phys.* **19**, 165 (1977).
- <sup>13</sup>R. C. Johnson and R. E. Merrifield, *Phys. Rev. B* **1**, 896 (1970).
- <sup>14</sup>M. O. Scully and W. E. Lamb Jr., *Phys. Rev.* **159**, 208 (1967).
- <sup>15</sup>R. Haberkorn, *Molec. Phys.* **32**, 1491 (1976).
- <sup>16</sup>K. L. Ivanov, M. V. Petrova, N. N. Lukzen, and K. Maeda, *J. Chem. Phys. A* **114**, 9447 (2010).
- <sup>17</sup>H. Hayashi, *Introduction to Dynamic Spin Chemistry: MFE and Biochemical Reactions*, in Vol. 8 of Lecture and Course Notes in Chemistry Series (World Scientific, Singapore, 2004).
- <sup>18</sup>U. E. Steiner and T. Ulrich, *Chem. Rev.* **89**, 51 (1989).
- <sup>19</sup>K. Schulten and P. G. Wolynes, *J. Chem. Phys.* **68**, 3292 (1978).
- <sup>20</sup>W. Wagemans, A. J. Schellekens, M. Kemper, F. L. Bloom, P. A. Bobbert, and B. Koopmans, *Phys. Rev. Lett.* **106**, 196802 (2011).
- <sup>21</sup>T. D. Nguyen, G. Hukic-Markosian, F. Wang, L. Wojcik, X.-G. Li, E. Ehrenfreund, and Z. V. Vardeny, *Nat. Mater.* **9**, 345 (2010).
- <sup>22</sup>F. L. Bloom, W. Wagemans, M. Kemerink, and B. Koopmans, *Phys. Rev. Lett.* **99**, 257201 (2007).
- <sup>23</sup>W. Wagemans, P. Janssen, A. J. Schellekens, F. L. Bloom, P. A. Bobbert, and B. Koopmans, *J. SPIN*, 2011 (accepted).
- <sup>24</sup>S. P. Kersten, A. J. Schellekens, B. Koopmans, and P. A. Bobbert, *Phys. Rev. Lett.* **106**, 197402 (2011).
- <sup>25</sup>T. D. Nguyen, B. R. Gautam, E. Ehrenfreund, and Z. V. Vardeny, *Phys. Rev. Lett.* **105**, 166804 (2010).
- <sup>26</sup>Z. Xu and B. Hu, *Adv. Funct. Mater.* **18**, 2611 (2008).
- <sup>27</sup>S. P. Kersten, A. J. Schellekens, B. Koopmans, and P. A. Bobbert, *Syn. Metals 2010* (article in press).
- <sup>28</sup>J. D. Bergeson, V. N. Prigodin, D. M. Lincoln, and A. J. Epstein, *Phys. Rev. Lett.* **100**, 067201 (2008).
- <sup>29</sup>M. J. Hansen, and J. B. Pedersen, *Chem. Phys. Lett.* **361**, 219 (2002).
- <sup>30</sup>Ö. Mermer, G. Veeraraghavan, T. L. Francis, Y. Sheng, D. T. Nguyen, M. Wohlgenannt, A. Köhler, M. K. Al Suti, and M. S. Khan, *Phys. Rev. B* **72**, 205202 (2005).
- <sup>31</sup>Y. Sheng, D. T. Nguyen, G. Veeraraghavan, Ö. Mermer, M. Wohlgenannt, S. Qiu, and U. Scherf, *Phys. Rev. B* **74**, 045213 (2006).
- <sup>32</sup>C. F. O. Graeff, G. B. Silva, F. Nüesch, and L. Zuppiroli, *Eur. Phys. J. E* **18**, 21 (2005).
- <sup>33</sup>R. C. Johnson, R. E. Merrifield, P. Avakian, and R. B. Flippen, *Phys. Rev. Lett.* **19**, 285 (1967).
- <sup>34</sup>I. V. Tolstov, A. V. Belov, M. G. Kaplunov, I. K. Yakuschenko, N. G. Spitsina, M. M. Triebel, and E. L. Frankevich, *J. Lumin.* **112**, 368 (2005).
- <sup>35</sup>T.-H. Lee, T.-F. Guo, J. C. A. Huang, and T.-C. Wen, *Appl. Phys. Lett.* **92**, 153303 (2008).
- <sup>36</sup>H. Bouchriha, G. Delacote, P. Delannoy, and M. Schott, *J. Phys.* **35**, 577 (1974).
- <sup>37</sup>M. A. Baldo, D. F. O'Brien, Y. You, A. Shoustikov, S. Sibley, M. E. Thompson, and S. R. Forrest, *Nature (London)* **395**, 151 (1998).
- <sup>38</sup>S. Blumstengel, F. Meinardi, R. Tubino, M. Gurioli, M. Jandke, and P. Strohhriegl, *J. Chem. Phys.* **115**, 3249 (2001).
- <sup>39</sup>V. Ern and R. E. Merrifield, *Phys. Rev. Lett.* **21**, 609 (1968).
- <sup>40</sup>J. Godlewski, G. Jarosz, and R. Signerski, *Appl. Surf. Sci.* **175**, 344 (2001).
- <sup>41</sup>J. Y. Song, N. Stingelin, W. P. Gillin, and T. Kreouzis, *Appl. Phys. Lett.* **93**, 233306 (2008).
- <sup>42</sup>B. Kirste, H. Van Willigen, H. Kurreck, K. Möbius, M. Plato, and R. Biehl, *J. Am. Chem. Soc.* **100**, 7505 (1978).
- <sup>43</sup>P. Avakian, R. P. Groff, R. E. Kellogg, R. E. Merrifield, and A. Suna, in *Organic Scintillators and Liquid Scintillation Counting* (Academic, New York, 1971).
- <sup>44</sup>J. Y. Song, N. Stingelin, A. J. Drew, T. Kreouzis, and W. P. Gillin, *Phys. Rev. B* **82**, 085205 (2010).
- <sup>45</sup>K. Lendi, P. Gerber, and H. Labhart, *Chem. Phys.* **175**, 449 (1976).
- <sup>46</sup>J. Mezyk, R. Tubino, A. Monguzzi, A. Mech, and F. Meinardi, *Phys. Rev. Lett.* **102**, 087404 (2009).
- <sup>47</sup>A. Suna, *Phys. Rev. B* **1**, 1716 (1970).
- <sup>48</sup>F. L. Bloom, M. Kemerink, W. Wagemans, and B. Koopmans, *Phys. Rev. Lett.* **103**, 066601 (2009).